JMEPEG (2011) 20:1023–1027
DOI: 10.1007/s11665-010-9716-z

1059-9495/$19.00

Fatigue Behavior of Vitallium-2000 Plus Alloy for Orthopedic Applications

K.V. Sudhakar and Jyhwen Wang

(Submitted January 7, 2010; in revised form May 21, 2010)

Vitallium-2000 Plus alloy is one of the important metallic biomaterials having excellent biocompatibility as it is free from nickel, vanadium, and beryllium elements that could cause potential allergic problems to patients. In this study, the high cycle fatigue behavior of continuous cast vitallium-2000 Plus alloy was investigated using rotation bend fatigue tests at 50 Hz frequency and at room temperature apart from tensile studies. A series of tests were carried out at varying stresses, and the S-N curve was obtained from regression of the test data. The endurance limit was determined as 387 MPa, which is very good for a cast alloy. This increase in fatigue property (compared to the previous version of this alloy) is primarily due to the presence of nitrogen that is added during continuous casting process and also that of the other alloying elements. Tensile test was also performed as per the ASTM standard to evaluate its static properties. The fracture morphology was investigated using scanning electron microscope to study the mechanisms of fracture. It was established that the primary mechanism of fracture was by microvoid nucleation and coalescence, typical of a ductile material that is significant for a cast alloy. The experimentally determined values of endurance limit, yield strength, tensile strength, and percent elongation provide evidence that vitallium-2000 Plus cast alloy has very good fatigue, tensile properties, and increased formability without fracture, allowing for excellent adjustability during its application.

Keywords endurance limit, fatigue behavior, fracture morphology, orthopedic applications, vitallium-2000 Plus alloy

1. Introduction

The most important metallic biomaterials are stainless steels, cobalt-chrome alloys, and titanium alloys. Metallic biomaterials are mainly used for replacing failed hard tissue and for dental applications. Stainless steel was first used successfully as an implant material in the surgical field when aseptic surgery was established and a cobalt-chrome alloy was implemented for practical applications. Cobalt-chrome alloys are typically used to fix soft tissue, such as blood vessels. The population ratio of the aged people worldwide is rapidly growing where the number of the aged people requiring replacement of failed tissue with metallic biomaterials is also growing. Hence, the development of metallic materials for biomedical applications has assumed a great importance (Ref 1).

Cobalt-chrome-based alloys are widely used in total hip and knee replacements, dental devices, and support structures for heart valves due to their excellent properties in terms of corrosion resistance, fatigue strength/endurance limit, and biocompatibility (Ref 2-5). Fatigue fracture and wear mechanisms are usually associated with implant failure of medical devices such as hip joint prostheses. The actual in vivo mechanisms are complex and involve the hostile body environment. They can be fatal in mechanical heart valves. An orthopedic device is an artificial mechanical device that replaces or supports part of the skeletal structure of the human body. One of the applications include internal fixation of fractures by bone plates, nails, or intermedular rods typically used as screws/plates for fixing fractured bones. The load on implant varies with position during walking and reaches a peak of about four times the body weight at the hip and three times the body weight at the knee. Furthermore, larger loads are experienced by the hip and knee joints during activities such as running and jumping. Regarding biocompatibility, cobalt-based alloys are highly resistant to corrosion, and especially to attack by chloride ions within crevice. Corrosion-related failure mechanism in a vitallium plate used as a fixation device has been investigated (Ref 6). High endurance limit/fatigue limit and good level of fracture toughness are considered as other relatively important advantages of vitallium alloy (Ref 7-9). Vitallium-2000 Plus alloy is known to provide improved physical and mechanical properties in comparison to other previous (vitallium and vitallium-2000) chrome-cobalt alloys.

Zhuang and Langer (Ref 10) investigated the effects of modifying the composition of the Co-Cr-Mo alloy with additions of nickel and some trace elements of aluminum, titanium, and boron. They observed a great improvement in the fatigue crack growth resistance of the cast alloy due to nickel additions to the base alloy. In addition, the fatigue fracture ductility was observed to be improved significantly with the nickel additions. It is also indicated that minor additions of such elements as aluminum, titanium, and boron contributed to improved fatigue crack growth resistance due to the reduction/elimination of some casting defects. Matkovic et al. (Ref 11) examined the influence of nickel and molybdenum addition

K.V. Sudhakar, Department of Metallurgical & Materials Engineering, Montana Tech of the University of Montana, Butte, MT 59701-8997; and **Jyhwen Wang**, Department of Engineering Technology & Industrial Distribution, Texas A&M University, College Station, TX 77843-3367. Contact e-mails: kvsudhakar@mtech.edu and Wang@entc.tamu.edu.

on the microstructural properties of as-cast Co-Cr-based alloys. The alloys were produced by vacuum arc-melting technique. It was established that among the 10 samples of Co-Cr-Ni alloys, only two samples with the composition $Co_{55}Cr_{40}Ni_5$ and $Co_{60}Cr_{30}Ni_{10}$ had appropriate dendritic solidification microstructure. This microstructure is known to be typical for commercial dental alloys. The results of hardness and corrosion resistance measurements revealed the strong influence of different alloy chemistry and of as-cast microstructure.

Hiromoto et al. (Ref 12) examined the corrosion behavior and microstructure of low-nickel Co-29Cr-7Mo alloys and a conventional Co-29Cr-6Mo-1Ni alloy (ASTM F75-92) in saline solution, Hanks' solution, and cell culture medium. The forging ratios of the Co-29Cr-6Mo alloy were 50 and 88% and that of the Co-29Cr-8Mo alloy was 88%. They found that the passive current densities of the low-nickel alloys were of the same order of magnitude as that of the ASTM alloy in all the solutions. The anodic current densities in the secondary passive region of the low-nickel alloys were lower than that of the ASTM alloy in the cell culture medium. Consequently, the low-nickel alloys were expected to show the same high corrosion resistance as the ASTM alloy. On the other hand, the passive current density of the Co-29Cr-6Mo alloy with a forging ratio of 50% was slightly lower than that of the alloy with a forging ratio of 88% in the saline. It was concluded that the refining of grains by forging further caused the increase in the passive current density of the low-nickel alloy.

Kurosu et al. (Ref 13) investigated the mechanical properties of Co-29Cr-6Mo alloys consisting of ε and σ phases at room temperature. Solution treatment at 1523 K for 7.2 ks was carried out for cast Co-29Cr-6Mo alloy, followed by various aging treatments at 1023 K for up to 21.6 ks. They found that 0.2% proof strength, ultimate tensile strength, and plastic elongation of the aged alloys did not depend on the aging time. Dourandish et al. (Ref 14) produced complex-shaped bimetals utilizing two-color powder injection molding (2C-PIM) and three-dimensional printing (3DP) processes, which basically involved sintering of a powder/binder mixture. They addressed the sintering of biocompatible Co-Cr-Mo alloy for producing stepwise porosity-graded composite structures. Such composite structures provide strength at the core and a porous layer for the tissue growth. It was found that an intermediate sintering temperature of 1280 °C in argon atmosphere can be used for manufacturing of the porosity-graded composite layers. They produced a hip-joint with a core/shell structure as a case study.

Lee et al. (Ref 15) observed an improvement in the mechanical properties of a biomedical nickel-free Co-Cr-Mo alloy in the as-cast condition using tensile tests and microstructure observations. They found that the solubility of nitrogen in Co-Cr-Mo alloys increased as the chromium content was increased from 29 to 34 mass%. This resulted in a significant improvement in mechanical properties such as yield stress, tensile strength, and fracture elongation. Increasing the chromium content also had contributed to the improved mechanical properties. Investigation of wrought Co-Cr-Mo implant alloy (Ref 16), which included studying the effect of iron addition on microstructures and mechanical properties of nickel- and carbon-free Co-Cr-Mo alloys (Ref 17), and the modification of mechanical properties of sintered implant materials in Co-Cr-Mo alloy (Ref 18) were also referred to assess the latest development on vitallium alloys.

Based on the above review, it was determined that rotating bending studies would provide new information on fatigue of vitallium-2000 Plus alloy (latest grade of Co-Cr-Mo alloy). The specific objectives of this investigation are evaluating the endurance/fatigue limit for this alloy and tensile properties in addition to characterizing their fracture morphology and comparing these properties with the previous vitallium alloy.

2. Experimental Procedure

2.1 Material and Heat Treatment

Vitallium-2000 Plus implants (intermedular nails and plain pattern bone plate) are shown (Fig. 1 and 2, respectively). The segmental fracture of the tibia, bridged by an intramedular nail with a proximal interlocking screw is depicted in Fig. 3. The chemical composition of vitallium-2000 Plus alloy and that of the previous (cast vitallium) alloy are detailed in Table 1. The vitallium-2000 Plus alloy investigated in this study incorporated an addition of controlled nitrogen during the continuous casting process, which is expected to result in higher values of yield, tensile strength, and percent elongation than any other chrome-cobalt alloys. This alloy was continuously cast and annealed at 1200 °C.

2.2 High Cycle (Rotating Cantilever Beam Test) Fatigue Test

The fatigue specimens (5-mm gage diameter and 20-mm gage length with a continuous radius) were machined from round bars (having the same properties as that of vitallium-200 Plus implants). The high cycle fatigue test was carried out at 3000 rpm and room temperature. Two specimens were tested to generate each data point on the S-N curve.

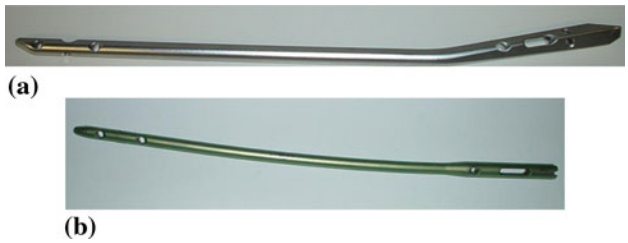

Fig. 1 (a, b) Intermedular nails

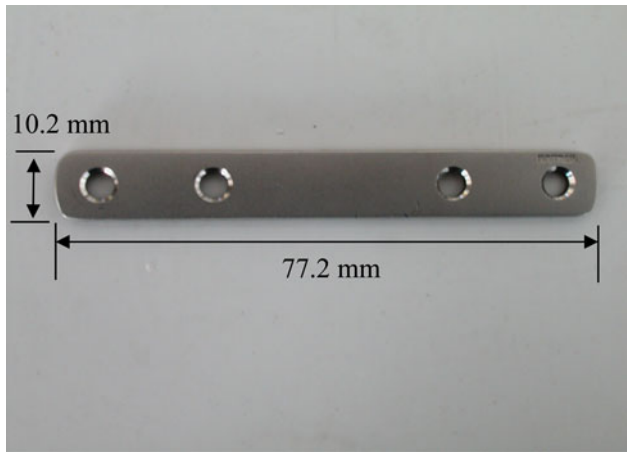

Fig. 2 Vitallium-2000 plain pattern bone plate

In rotating cantilever beam fatigue test, one end of a machined specimen is mounted in a motor-driven chuck. A known weight is suspended at a distance from the support. The top surface of the test specimen is subjected to tensile force, while the bottom surface is compressed. After the specimen turns 90°, the locations that were originally in tension and compression have no stress acting on them. After a half revolution of 180°, the material that was originally in tension is now in compression. Thus, the stress at any one point goes through a complete sinusoidal cycle from maximum tensile stress to maximum compressive stress. An R. R. Moore fatigue tester was used to conduct the experiments. The maximum stress (σ) acting on this type of specimen is given by the following equation:

$$\sigma = \pm\frac{32M}{\pi \cdot d^3} \quad \text{(Eq 1)}$$

where M is the bending moment, and d is the specimen diameter. The bending moment under the fatigue tester setup is:

$$M = \frac{F \cdot L}{2} \quad \text{(Eq 2)}$$

where F is the applied load, and L is the length of the specimen. The stress induced by bending in Eq 1 can be expressed as

$$\sigma = \pm\frac{16F \cdot L}{\pi \cdot d^3} \quad \text{(Eq 3)}$$

Fig. 3 A general picture showing segmental fracture of the tibia, bridged by an intramedular nail with a proximal interlocking screw

Vitallium-2000 Plus alloy (cobalt-chrome alloy) specimens were machined from round bars (having the same properties as those of vitallium-200 Plus alloy implants) to form fatigue test specimens with a continuous radius. These specimens having continuous radius were metallographically polished to have a smooth surface (high level of surface finish). This is basically to avoid the most likely influence of surface irregularities or roughness (at the microscopic level) on fatigue strength. The tests were carried out up to 10^7 cycles to determine the fatigue/endurance limit. The fatigue data are presented by the S-N curve where the stress S is plotted against the number of cycles to failure N.

2.3 Microhardness and Tensile Tests

Microhardness and tensile tests on vitallium-2000 Plus alloy were performed as per E384-06 and E8-04 ASTM standard Test Methods, respectively. Microhardness test was carried out at 100-g load and using the microhardness Vicker's diamond pyramid indenter. Tensile tests were carried out at a strain rate of about 0.001/s.

3. Results and Discussion

3.1 Microhardness and Tensile Properties

Microhardness test was carried out on the samples of vitallium plate and nail bones. From the microhardness measurements, the Vickers hardness (at 100-g load) of vitallium-2000 Plus alloy was experimentally determined as VHN 410 (average of 5 readings). The specimens were prepared to determine the tensile properties (average of 3 readings). The experimentally determined values for 0.2% proof stress, tensile strength, and elongation were 612 MPa, 824 MPa, and 15.2%, respectively. These tensile properties were higher as compared with the previous alloy of vitallium as reported in Table 1. The higher values of tensile properties are largely due to the presence of nitrogen element and also the combined effects of specific elements in this alloy that are known to minimize the microstructural casting defects (Ref 10).

3.2 High Cycle Fatigue Behavior

Various mechanical properties including the fatigue property are listed in Table 2 that also includes the comparison of the values with respect to the previous alloy. From the rotating beam test, the prescribed stress versus number of cycles to failure is shown in Fig. 4(a) which can be described by the Basquin equation:

$$N\sigma^p = C \quad \text{(Eq 4)}$$

where σ is the stress amplitude, and p and C are the constants that can be obtained from curve fitting. It can be

Table 1 Chemical composition (wt.%) of vitallium cast alloys

Elements	Co	Cr	Mo	Mn	Ni	C	Fe	Si	N
Vitallium-2000 Plus	65.0	29.5	5.4	0.05	1.2	0.2	0.28	0.8	0.1
Cast vitallium (a) (typical)	61.0	28.5	6.0	…	2.5	0.36 (max)	0.75	1.0% (max)	…

(a) Ref 20

Table 2 Mechanical properties of vitallium alloys

Properties	0.2%YS, MPa	UTS, MPa	Elongation, %	Microhardness, VHN_{100}	Fatigue limit, MPa
Vitallium-2000 Plus	612	824	15.2	410	387
Cast vitallium (a) (typical)	520	790	15.0	…	310

(a) Ref 20

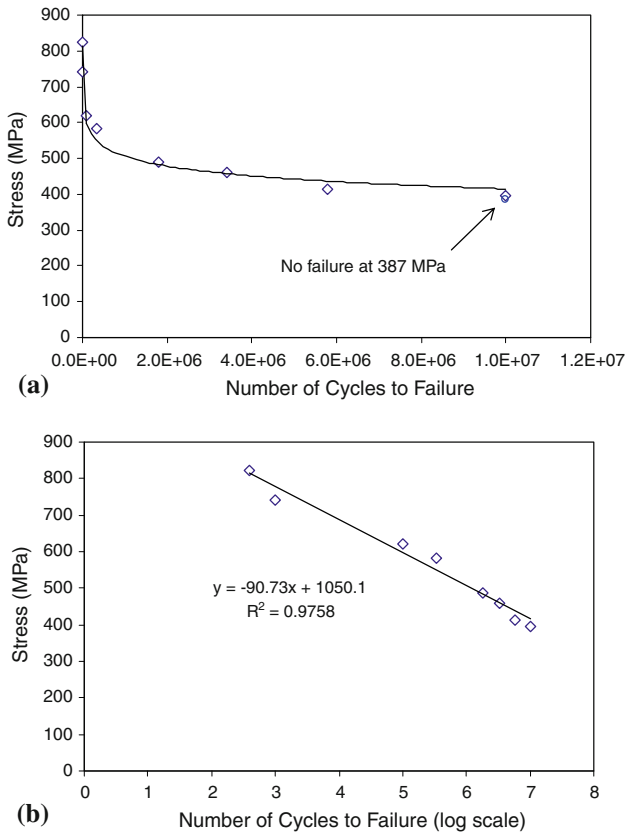

Fig. 4 (a, b) Fatigue behavior in terms of S-N curve and in log scale

observed that at higher stresses, the fatigue life is progressively decreased. With a prescribed stress of 396 MPa, fatigue failure occurred at around 10^7 cycles of loading. While no clear fatigue limit is observed, the experimental results showed that vitallium-2000 Plus alloy specimen exhibited a maximum stress of 387 MPa where there was no failure (fracture) at 10^7 cycles of loading. The high cycle behavior of the material is demonstrated in terms of an S-N curve as shown in Fig. 4(b). The linear regression of the experimental data in logarithm scale showed a strong relationship between the number of cycles to failure and the applied stress with $R^2 = 0.976$. The fatigue strength of vitallium-2000 Plus alloy can be described by the regression equation:

$$\sigma = -90.73(\log N) + 1050.1 \quad \text{(Eq 5)}$$

Based on Eq 5, the predicted failure stress at 10^7 cycles of loading is 415 MPa, which is very close to the experimental observation of 387 MPa. However, it should be noted that while conducting fatigue experiments, each specimen has its

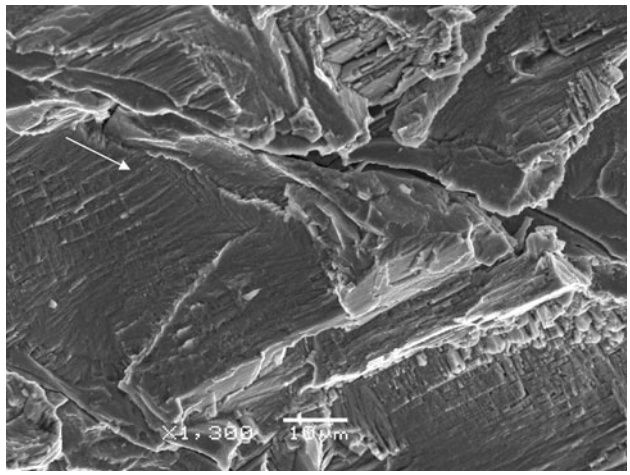

Fig. 5 The presence of a long fatigue crack (arrow indicates the crack growth direction) across the slip bands

own fatigue limit. Thus, fatigue life and fatigue limit are statistical quantities (Ref 19). The experimentally determined fatigue value of 387 MPa is a significant improvement in comparison to that of 310 MPa for a typical cast vitallium alloy (Ref 20), which is reported in Table 2. This improvement in fatigue property is primarily attributed to the specific composition (in particular the combination of cobalt and chromium elements) of the alloy, and improved microstructure thereby reducing the microstructural casting defects (Ref 10). Furthermore, the addition of nitrogen element during continuous casting of vitallium-2000 Plus alloy basically helped in contributing to its improved mechanical properties, including fatigue behavior (Ref 15).

3.3 Mechanisms of Crack Initiation and Propagation

The presence of a long fatigue crack is exhibited in Fig. 5 where the direction of the fatigue crack growth is clearly across the slip bands. The fracture surface during crack propagation demonstrating a highly ductile fracture with microvoids is shown in Fig. 6.

Vitallium-2000 Plus alloy demonstrated a typical ductile fracture. Ductile fracture is characterized by plastic deformation which precedes failure of the material. Upon close examination of the fracture surface, we can very clearly see a fibrous pattern with dimples. This kind of ductile fracture is initiated with the formation of tiny/micro voids, usually around small inclusions or preexisting voids. These microvoids then grow and coalesce, developing into cracks that grow in size and lead to fracture. Dimple size and shape depend on the type of loading and extent of microvoid emergence. When a material is subjected to uniaxial tensile loading, equiaxed dimples appear that have

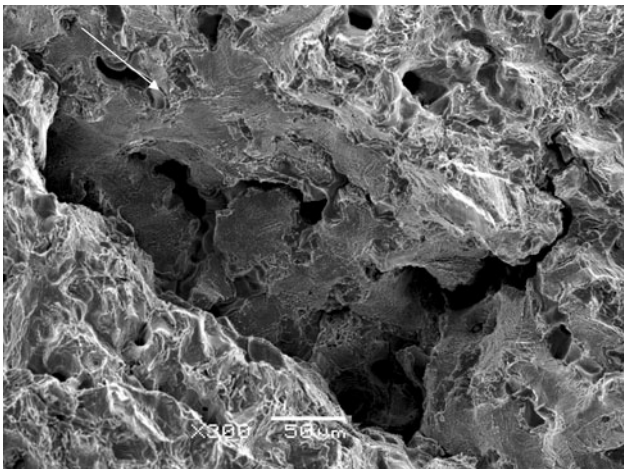

Fig. 6 Fracture surface at the crack propagation (arrow indicates the crack growth direction) demonstrating a highly ductile fracture with microvoids

complete rims. Under a tear loading, the dimples are elongated, the rims of the dimples are not complete, and the dimples are in the same direction as the loading. Intergranular dimple rupture occurs along grain boundaries due to nucleation and coalescence of voids at grain boundaries.

4. Conclusions

- The fatigue behavior of the vitallium-2000 Plus alloy can be described by a typical S-N curve with a good linear regression fit. This linear regression analysis could potentially save on time and effort to predict the stress-life at 10^7 cycles.
- Vitallium-2000 Plus alloy exhibited good level of endurance limit of 387 MPa (especially for a cast alloy) which makes it an attractive biomedical alloy requiring good dynamic characteristics. This is in addition to its relatively higher level of tensile properties. These values are higher than that for a previously cast vitallium alloy.
- The primary mechanism of failure in vitallium-2000 Plus alloy is typically that of ductile fracture with microvoid formation and coalescence demonstrating a good degree of toughness. This observation is significant especially for a cast alloy that supports the flexibile characteristic of this alloy in dental/orthopedic applications.
- The improved mechanical properties of vitallium-2000 Plus alloy with relatively higher levels of strength and fracture resistance are very beneficial in certain applications (dental/orthopedic) without excessive deformation or fracture.

References

1. M. Niinomi, Recent Metallic Materials for Biomedical Applications, *Metall. Mater. Trans.*, 2002, **33A**, p 477–486
2. D. Granchi, G. Ciapetti, S. Stea, L. Savarino, F. Filippini, A. Sudanese, G. Zinghi, and L. Montanaro, Cytokine Release in Mononuclear Cells of Patients with Co-Cr Hip Prosthesis, *Biomaterials*, 1999, **20**(12), p 1079–1086
3. B.Y. Li, A. Mukasyan, and A. Varma, Combustion Synthesis of Co-Cr-Mo Orthopedic Implant Alloys: Microstructure and Properties, *Mater. Res. Innov.*, 2003, **7**(4), p 245–252
4. E.L. Que, L.D.T. Topoleski, and N.L. Parks, Surface Roughness of Retrieved Co-Cr-Mo Alloy Femoral Components from PCA Artificial Total Knee Joints, *J. Biomed. Mater. Res.*, 2000, **53**(1), p 111–118
5. S.K. Yen and S.W. Hsu, Electrolytic Al_2O_3 Coating on Co-Cr-Mo Implant Alloys of Hip Prosthesis, *J. Biomed. Mater. Res.*, 2001, **54**(3), p 412–418
6. K.V. Sudhakar, Investigation of Failure Mechanism in Vitallium-2000 Implant, *Eng. Fail. Anal.*, 2005, **12**(2), p 257–262
7. A.G. Della Valle, B. Becksac, J. Anderson, T. Wright, B. Nestor, P.M. Pellicci, and E.A. Salvati, Late Fatigue Fracture of a Modern Cemented [Corrected] Cobalt Chrome Stem for Total Hip Arthroplasty: A Report of 10 Cases, *J. Arthroplasty*, 2005, **20**(8), p 1084–1088
8. E.W. Lee and H.T. Kim, Early Fatigue Failures of Cemented, Forged, Cobalt-Chromium Femoral Stems at the Neck-Shoulder Junction, *J. Arthroplasty*, 2001, **16**(2), p 236–238
9. S.T. Woolson, J.P. Milbauer, J.D. Bobyn, S. Yue, and W.J. Maloney, Fatigue Fracture of a Forged Cobalt-Chromium-Molybdenum Femoral Component Inserted with Cement, *J. Bone Joint Surg. Am.*, 1997, **79**(12), p 1842–1848
10. L.Z. Zhuang and E.W. Langer, Effects of Alloy Additions on the Fatigue Properties of Cast Co-Cr-Mo Alloy Used for Surgical Implants, *Mater. Sci.*, 1990, **25**(1B), p 683–689
11. T. Matkovic, P. Matkovic, and J. Malina, Effects of Ni and Mo on the Microstructure and Some Other Properties of Co-Cr Dental Alloys, *J. Alloys Compd.*, 2004, **366**(1–2), p 293–297
12. S. Hiromoto, E. Onodera, A. Chiba, K. Asami, and T. Hanawa, Microstructure and Corrosion Behavior in Biological Environments of the New Forged Low-Ni Co-Cr-Mo Alloys, *Biomaterials*, 2005, **26**(24), p 4912–4923
13. S. Kurosu, N. Nomura, and A. Chiba, Microstructure and Mechanical Properties of Co-29Cr-6Mo Alloy Aged at 1023 K, *Mater. Trans.*, 2007, **48**(6), p 1517–1522
14. M. Dourandish, D. Godlinski, A. Simchi, and V. Firouzdor, Sintering of Biocompatible P/M Co-Cr-Mo Alloy (F-75) for Fabrication of Porosity-Graded Composite Structures, *Mater. Sci. Eng. A*, 2008, **472**(1–2), p 338–346
15. S.-H. Lee, N. Nomura, and A. Chiba, Significant Improvement in Mechanical Properties of Biomedical Co-Cr-Mo Alloys with Combination of N Addition and Cr-Enrichment, *Mater. Trans.*, 2008, **49**(2), p 260–264
16. S.-H. Lee, E. Takahashi, N. Nomura, and A. Chiba, Effect of Carbon Addition on Microstructure and Mechanical Properties of a Wrought Co-Cr-Mo Implant Alloy, *Mater. Trans.*, 2006, **47**(2), p 287–290
17. S.-H. Lee, N. Nomura, and A. Chiba, Effect of Fe Addition on Microstructures and Mechanical Properties of Ni- and C-Free Co-Cr-Mo Alloys, *Mater. Trans.*, 2007, **48**(8), p 2207–2211
18. M. Grazka-Dahlke, J.R. Dabrowski, and B. Dabrowski, Modification of Mechanical Properties of Sintered Implant Materials on the Base of Co-Cr-Mo Alloy, *J. Mater. Process. Technol.*, 2008, **204**(1–3), p 199–205
19. G.E. Dieter, *Mechanical Metallurgy*, McGraw-Hill, 1986
20. M. Donachie, *Metals Handbook*, Desk edition, 2nd ed., ASM International, Materials Park, OH, 2008, p 702–709